

# Local Structure of $\text{La}_{1-x}\text{Sr}_x\text{CoO}_3$ determined from EXAFS and neutron PDF studies

N. Sundaram<sup>1</sup>, Y. Jiang<sup>1</sup>, I.E. Anderson<sup>1</sup>, D.P. Belanger<sup>1</sup>,

C.H. Booth<sup>2</sup>, F. Bridges<sup>1</sup>, J.F. Mitchell<sup>3</sup>, Th. Proffen<sup>4</sup>, H. Zheng<sup>3</sup>

<sup>1</sup>*Department of Physics, University of California, Santa Cruz, CA 95064, USA*

<sup>2</sup>*Chemical Sciences Division, Lawrence Berkeley National Laboratory, 1 Cyclotron Rd. Berkeley, CA 94720, USA*

<sup>3</sup>*Materials Science Division, Argonne National Laboratory, 9700 Cass Ave, Argonne, IL 60439, USA and*

<sup>4</sup>*Lujan Neutron Scattering Center, Los Alamos National Laboratory, Los Alamos, NM 87545, USA*

The combined local structure techniques, extended x-ray absorption fine structure (EXAFS) and neutron pair distribution function analysis, have been used for temperatures  $4 \leq T \leq 330$  K to rule out a large Jahn-Teller (JT) distortion of the Co-O bond in  $\text{La}_{1-x}\text{Sr}_x\text{CoO}_3$  for a significant fraction of Co sites ( $x \leq 0.35$ ), indicating few, if any, JT-active, singly occupied  $e_g$  Co sites exist.

The cobaltite system  $\text{La}_{1-x}\text{Sr}_x\text{CoO}_3$  (LSCO) has a rich temperature-concentration phase diagram as a result of multiple relevant energy scales. In the parent compound,  $\text{LaCoO}_3$  (LCO), a significant thermal population of an excited spin state occurs above  $T = 100$  K [1]. Models generally include a low spin state (LS,  $S = 0$ ) at low  $T$ , with electronic configuration  $t_{2g}^6 e_g^0$ , along with either an intermediate spin (IS,  $S = 1$ ),  $t_{2g}^5 e_g^1$ , or a high spin state (HS,  $S = 2$ ),  $t_{2g}^4 e_g^2$ , that becomes populated as  $T$  increases. Since the theoretical work of Potze *et al.* [2], and Korotin *et al.* [3], which developed ideas by Goodenough [4] and Zaanen *et al.* [5], the IS state has often been invoked for interpreting experimental results at intermediate  $T$  in LCO and LSCO. More recently, the theoretical support for the IS has been questioned [6]. An excellent review is given by Medarde, *et al.* [7]. The IS state is expected to be Jahn-Teller (JT) active, with local distortions of the O octahedra surrounding the Co ions, breaking the 6-fold symmetry and creating Co-O bonds with different lengths. The related  $\text{La}_{1-y}\text{Ca}_y\text{MnO}_3$  (LCMO) manganite system exhibits a large JT distortion of the Mn-O bonds as reported in several recent extended x-ray absorption fine structure (EXAFS) and neutron pair distribution function (PDF) studies [8–10]. A similar distortion has been found in  $\text{La}_{1-x}\text{Sr}_x\text{MnO}_3$  (LSMO) by Louca *et al.*, [11] (PDF), while Mannella *et al.*, [12] (EXAFS) report a smaller distortion for LSMO.

If the proposed IS state is present in LCO, then it should exhibit the associated JT distortion with a split Co-O bond peak for  $T > 100$  K but not for  $T \ll 100$  K. The larger Sr ion decreases the crystal field splitting, which would be expected to enhance the IS state [13]. Previous magnetic susceptibility work [14] shows that in LSCO the excited spin state persists to low  $T$ . Hence, at low  $T$  we should see no split peak for LCO, followed by increasing evidence for a splitting with increasing doping. More importantly, a splitting should exist at  $T = 300$  K for all concentrations if the IS state is the operative one.

Previous neutron PDF studies of LSCO [15] indicated a local distortion comparable to LSMO with four short and two long Co-O bonds. However, while some recent experimental results [15, 16] are argued to be consistent

with a large JT distortion and its associated IS, with the recent work of Klie *et al.* [17] claiming to exclude a transition to the HS state, others [7, 18, 19] are argued to be inconsistent with an LS-IS interpretation, but these are not local structure measurements. Here, we report neutron PDF and EXAFS results which show that the non-thermal local distortions in LSCO materials are, in fact, much smaller than those in LCMO.

Powder samples of  $\text{La}_{1-x}\text{Sr}_x\text{CoO}_3$  ( $x = 0, 0.15, 0.20, 0.25, 0.30, \text{ and } 0.35$ ) were synthesized by Mitchell and Zheng at ANL (MZ) and by Sundaram at UCSC (NS) using a standard solid state reaction [14]. Stoichiometric amounts of  $\text{La}_2\text{O}_3$ ,  $\text{SrCO}_3$  and  $\text{Co}_3\text{O}_4$  were ground thoroughly and fired several times at temperatures ranging from  $875^\circ\text{C}$  to  $1100^\circ\text{C}$  for several days, with a final heating at  $1200^\circ\text{C}$  for one day in air. X-ray diffraction measurements confirmed the formation of pure phase material and iodometric titrations or thermogravimetric analysis confirmed correct oxygen stoichiometry. Magnetization measurements at the Lawrence Berkeley National Laboratory are consistent with previous results [20].

Temperature dependent EXAFS transmission Co  $K$  edge data for the LSCO samples were collected at the Stanford Synchrotron Radiation Laboratory (SSRL). Fine powders were brushed onto tape; several tape layers were used to make the step height (the x-ray absorption increase at the Co  $K$  edge)  $0.3 \sim 0.5$ . The double Si (111) monochromator was detuned 50% to reduce harmonics. The energy resolution was  $\sim 1$  eV.

A standard data reduction was used to extract the EXAFS  $k$ -space oscillations, which were Fourier transformed into  $r$ -space (RSXAP package [21]). Next, the data were fit to theoretical EXAFS functions generated by FEFF 8.20 (Rehr and co-workers [22]), using the program `rsfit` (RSXAP package). Our primary interest here is  $\sigma$ , the width of the Co-O PDF, which parametrizes the amount of distortion present around the Co ions. Note that uncorrelated contributions to  $\sigma^2$  add in quadrature; *i.e.*  $\sigma_{total}^2 = \sigma_{static}^2 + \sigma_{phonons}^2 + \sigma_{Jahn-Teller}^2$ .

The thermal phonon contributions were determined from a fit of  $\sigma^2(T)$  vs.  $T$ , for  $4 \leq T \leq 330$  K, to the correlated Debye model plus a static off-set. This model

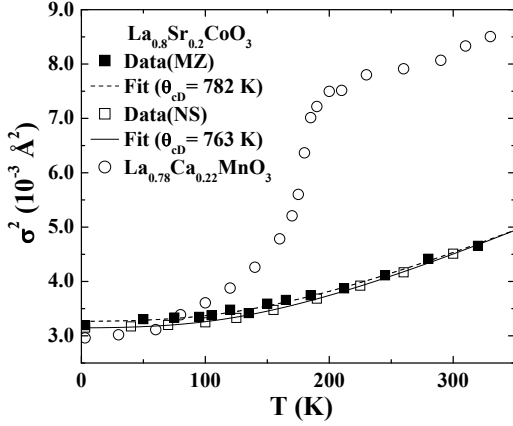


FIG. 1:  $\sigma^2(T)$  for the  $\text{La}_{0.8}\text{Sr}_{0.2}\text{CoO}_3$  MZ and NS samples, and correlated Debye fits. The data overlap very well within the relative errors that are comparable or smaller than the symbol sizes. Similar results for a  $\text{La}_{0.78}\text{Ca}_{0.22}\text{MnO}_3$  sample (Mn-O bond, see Ref. 9) are replotted here; this sample has a large JT distortion that develops between 100 and 200 K.

is usually a good approximation for all phonon modes [23] including acoustic and optical phonons [24, 25]; see Ref. [9] for details about our use of this model.

In Fig. 1 we plot  $\sigma^2(T)$  and the correlated Debye fits for MZ and NS  $\text{La}_{0.8}\text{Sr}_{0.2}\text{CoO}_3$  samples. The relative errors (Figs. 1 and 21) are comparable to the scatter in the data; systematic errors, which should be the same at all  $T$  for a given sample and nearly the same for all samples, are also present. Such errors, which shift the entire plot up or down on the vertical axis, are estimated to be less than  $5 \times 10^{-4} \text{ \AA}^2$ . We also plot, for comparison, corresponding results for a 22% Ca-doped LCMO sample [9] which has a metal-insulator (MI) transition around 190 K associated with a local JT distortion of the Mn-O octahedra. Between 100 and 200 K, the JT splitting results in a configuration with two longer Mn-O bonds and four relatively shorter bonds for some sites (at low  $T$ , the Mn-O octahedron has six bonds of nearly equal length). The proposed JT distortion of the Co-O bonds in LSCO [15] is of comparable magnitude to that observed in LCMO. However, the lack of any significant step for LSCO in Fig. 1 and the rather small static distortion at 4K ( $\leq 0.0006 \text{ \AA}^2$ ) indicates very little JT distortion of the Co-O PDF peak between 4 and 300 K for the 20% Sr doped LSCO samples. One cannot, of course, rule out the possibility of a few percent of sites having a JT distortion.

Fig. 2 shows  $\sigma^2(T)$  (Co-O peak) for two samples. The plots indicate that LCO has a slightly less distorted environment around the Co atoms; however, the difference in  $\sigma^2$  at 4 K between this sample and the others is comparable to the systematic uncertainty, so it is not a definitive result. For the 30% Sr sample [Fig. 2(b)], data from one experiment overlap well with those from an experiment one year earlier. These results together with the 20%

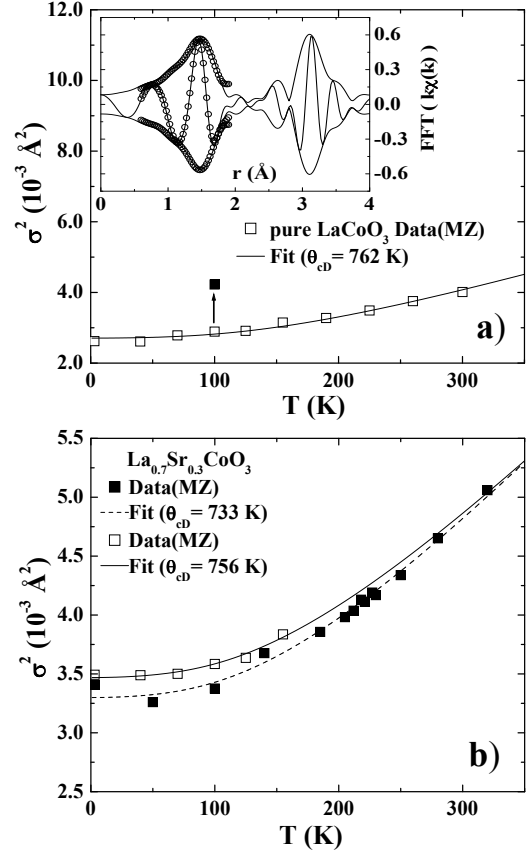


FIG. 2: a)  $\sigma^2(T)$  for  $\text{LaCoO}_3$  and the correlated Debye fit. The inset is an example of 4 K  $r$ -space data (solid line) and a fit to Co-O first peak (open circle); the Fourier Transform (FT) range is  $3.3 - 12.0 \text{ \AA}^{-1}$  with a Gaussian broadening of  $0.3 \text{ \AA}^{-1}$ , and the  $r$ -space fit range is  $1.1$  to  $1.7 \text{ \AA}$ . Note that we are fitting to the fast oscillating real and imaginary (not shown) parts of the FT. A good fit is obtained from  $0.7 - 1.8 \text{ \AA}$ . b)  $\sigma^2(T)$  for the  $\text{La}_{0.7}\text{Sr}_{0.3}\text{CoO}_3$  JM samples. The solid squares represent the data from the first measurement, and open squares represent the data from the second measurement showing consistency between measurements taken a year apart; the dashed line is the correlated Debye fit for the first experiment data, while the solid line is the fit for the second experiment data. The solid symbol in a) shows the increase in  $\sigma^2$  if a 3-peak splitting occurs near 100 K.

LSCO data in Fig. 1 show the consistency of the data collection and analysis.

The correlated Debye temperature ( $\theta_{cD}$ ) for all samples is approximately 760 K and is a measure of the Co-O bond strength. For this relatively high value of  $\theta_{cD}$  and the limited  $T$  range ( $T/\theta_{cD} < 0.4$ ),  $\theta_{cD}$  is strongly dependent on small fluctuations of the  $\sigma^2(T)$  data points, particularly at higher  $T$ ; thus this relatively large observed scatter in  $\theta_{cD}$  (see Figs. 1,2) is expected and the overall uncertainty is likely 30-40 K. For comparison  $\theta_{cD}$  for the Mn-O peak in LCMO is  $\sim 830 \text{ K}$  [9]. The static contribution,  $\sigma_{static}^2$ , obtained from these Debye fits, range from  $0.3 - 7.8 \times 10^{-4} \text{ \AA}^2$  for all our samples ( $0 \leq x \leq 0.3$ ).

The zero-point-motion contribution to  $\sigma^2$  for this value of  $\theta_{cD}$  is  $2.6 \times 10^{-3} \text{ \AA}^2$ . Hence, this static contribution is very small for all samples and consistent with  $\sigma_{static}^2 = 0$  within our systematic uncertainty,  $5 \times 10^{-4} \text{ \AA}^2$ .

There are three published EXAFS papers on the Sr doped cobaltites; however, they only report room temperature data [26, 27]. When fitting the first shell Co-O peak to a single Gaussian, they all obtain similar  $\sigma^2$  (300 K) results to those we report above. However, a diffraction study has suggested that a 3-peak splitting of the Co-O bonds develops above  $\sim 70$  K (space group change from  $R\bar{3}c$  to  $I2/a$ ,  $\Delta r \sim 0.05$ - $0.06 \text{ \AA}$ , although the change in the fit parameter for the two fits is very small)[28]. Two of the EXAFS groups therefore tried a split-peak fit and suggest a splitting of approximately  $0.06 \text{ \AA}$  [27], much smaller than the  $0.15 \text{ \AA}$  splitting reported by Louca *et al.*, [11]. However,  $0.06 \text{ \AA}$  is well below the Fourier limit for resolving a split peak in EXAFS when the maximum  $k$  is  $\sim 13$ - $14 \text{ \AA}^{-1}$ ; a split peak cannot be resolved if  $\Delta r < \frac{\pi}{2k_{max}}$  [24, 29].

For comparison with these other reports, we have also included the effect of a splitting of the Co-O peak into 3-peaks between 60 and 100 K. In that case for peaks at  $r$ ,  $r \pm \Delta r$ , there is an additional static contribution -  $\sigma_{static}^2 = 2/3(\Delta r)^2$  [24]. Using  $\Delta r = 0.05 \text{ \AA}$  and the zero-point-motion contribution above, the value of  $\sigma^2$  would increase to  $4.2 \times 10^{-3} \text{ \AA}^2$ , as shown by a solid point at 100K in Fig. 2(a); a simulation made using three such peaks, and fit using a single peak as for the data, yielded the same result. We would easily see a step change of this magnitude - it is inconsistent with the EXAFS data. An upper limit to a 3-peak splitting, using a possible step change in  $\sigma^2$  that is three times the scatter in the data, is  $\Delta r \leq 0.025 \text{ \AA}$ . Also if we assume a 3-peak JT splitting occurs at all T, an upper limit for such a splitting from the static contribution to  $\sigma^2$  is  $\Delta r \leq 0.03 \text{ \AA}$ ; assuming a 2-peak splitting model instead, the maximum  $\Delta r$  would be  $\approx 0.05 \text{ \AA}$ . Hence, any JT distortion at low  $T$  must be small, or the fraction of JT split sites less than 5-10%.

The neutron PDF technique is another local structure probe well suited for investigating JT splittings of the Co-O bonds [30], as long as the splitting is larger than the resolution and involves a significant number of Co sites. As discussed above, if the proposed IS state exists, then the LCO should exhibit a JT distortion with a split Co-O bond peak for  $T > 100$  K but not for  $T \ll 100$  K, while the doped compounds should show a splitting at all  $T$ . We collected neutron diffraction data for the NS samples using the high-resolution neutron powder diffractometer NPDF [31] at the Lujan Neutron Scattering Center, LANL. Data at  $T = 12, 100,$  and  $300$  K for each sample were corrected for detector dead time and efficiency, background, absorption, multiple scattering, and inelastic effects. The data were then normalized by the incident flux and the total sample scattering cross section to yield the total scattering structure function  $S(Q)$ , from which

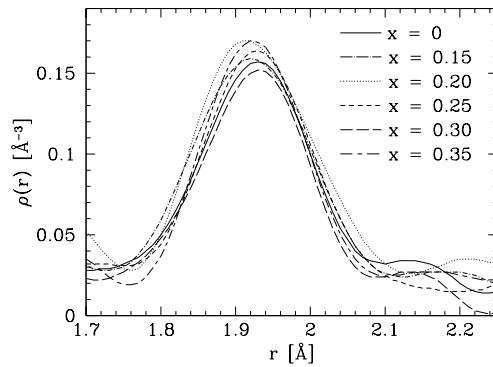


FIG. 3:  $\rho(r)$  for all the samples at  $T = 300$  K with  $Q_{max} = 35 \text{ \AA}^{-1}$ . The large peak represents a Co-O bond length of  $1.92 \text{ \AA}$ . There is little evidence for the peak previously reported [11] at  $2.15 \text{ \AA}$ .

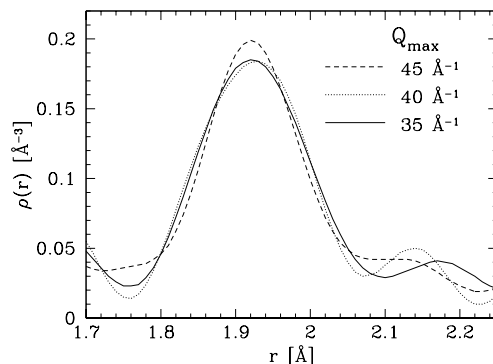


FIG. 4:  $\rho(r)$  obtained from the scattering data on LCO using different  $Q_{max}$  at  $T = 200$  K. Although a small peak can be seen between  $2.1$  and  $2.2 \text{ \AA}$ , its position changes with  $Q_{max}$  and does not indicate a real bond length in this  $r$  range.

the PDF,  $G(r)$ , and the pair density function,  $\rho(r)$ , were obtained by a Fourier transform [30]. Data were collected with reciprocal lattice vectors as large as  $Q = 45 \text{ \AA}^{-1}$ , giving a high real-space resolution  $\leq 0.1 \text{ \AA}$ . The program PDFGETN [32] was used for data processing.

Figure 3 shows no evidence for a split peak in the PDF data from any sample at  $T = 300$  K, nor is one observed at lower  $T$ . The small peak that seems to appear near  $2.15 \sim 2.2 \text{ \AA}$  is much smaller than the peak observed in earlier PDF measurements [11] at  $2.1 \text{ \AA}$ , and it shifts in  $r$  with changing values of  $Q_{max}$ , the maximum cutoff in  $Q$ , as exemplified by three different  $Q_{max}$  in Fig. 4 for the same set of data. The strong  $Q_{max}$  dependence demonstrates that the small peak does not represent a splitting from the main peak and hence, a JT distortion, but is primarily an effect of termination ripples [30] introduced in the Fourier transform by changes in  $Q_{max}$ . Peaks representing real structure are not sensitive to  $Q_{max}$ . It is clear that the position of the large Co-O peak at  $1.92 \text{ \AA}$  does not significantly change position.

Recent neutron PDF studies [33] of  $\text{La}_{1-y}\text{Ba}_y\text{CoO}_3$

and  $\text{La}_{1-y}\text{Ca}_y\text{CoO}_3$  indicated asymmetric Co-O peaks, particularly in the former compound, giving evidence for the IS state in these compounds. We observed no evidence of asymmetry in our LSCO data.

Rietveld refinements using the  $I2/a$  space group reported by Maris *et al.* [28] did not yield better fits of our data than the  $R\bar{3}c$  space group used by most other groups. Moreover, the three Co-O bond lengths found are well within 0.001 Å of each other. Using the Maris *et al.* results with a split first Co-O peak, we calculated the corresponding PDF; the results are not consistent with our data. We conclude that our data are fit better by the  $R\bar{3}c$  space group, as will be reported elsewhere.

Our neutron data show no evidence for a JT distortion in LCO or LSCO, in complete agreement with the EXAFS results described earlier. Together, our EXAFS and neutron PDF data indicate that, if the localized spin model with the LS  $\rightarrow$  IS scenario is operative, either the  $e_g$  state does not couple to the lattice as much as previously expected, resulting in undetectably small distortions, or it involves very few Co sites. This result should be considered in the interpretation of the low energy excitations observed in LSCO and LCO [34]. Recent experiments have been interpreted as being more compatible with a LS  $\rightarrow$  HS scenario, perhaps with inhomogeneous mixed-spin states and strong Co-O orbital hybridization [7, 18, 35]. Our combined local structure results remove an apparent contradiction between such measurements and earlier local structure results[15]. An important consideration is the hole hopping rate in conducting samples - if the hole hops faster than phonon time scales, the O atoms have no time to respond and no (or little) distortion will be observed: for example, very little distortion is observed for the CMR manganites at low  $T$  while a small JT distortion is observed in LSMO at high  $T$  where the polarons are hopping rapidly[12]. Using the localized spin models may be incomplete if the conducting charges have a wavefunction spread over several sites [36].

More extensive studies of  $\text{La}_{1-x}\text{Sr}_x\text{CoO}_3$  will be reported elsewhere, including results for bulk powders, such as those used here, and 20-40 nm nanoparticle powders.

Work at UCSC was partly funded by DOE Grant No. DE-FG02-05ER46181. Work at Argonne National Laboratory was supported by the US DOE, Office of Science, under Contract No. DE-AC-02-06CH11357. EXAFS experiments were performed at SSRL (operated by the DOE, Div. of Chemical Sciences, and by the NIH, Biomedical Resource Technology Program, Div. of Research Resources). This work has benefited from the use of NPDF at the Lujan Center, funded by DOE Office of Basic Energy Sciences (BES). Los Alamos National Laboratory is operated by Los Alamos National Security LLC under DOE Contract DE-AC52-06NA25396. Work at Lawrence Berkeley National Laboratory was supported by U. S. DOE, BES, under contract DE-AC02-05CH11231.

- 
- [1] K. Asai *et al.*, Phys. Rev. B **50**, 3025 (1994).
  - [2] R. H. Potze, G.A. Sawatzky, and M. Abbate, Phys. Rev. B **51**, 11501 (1995).
  - [3] M.A. Korotin *et al.*, Phys. Rev. B **54**, 5309 (1996).
  - [4] J.B. Goodenough, Mat. Res. Bull. **6**, 967 (1971).
  - [5] J. Zaanen, G.A. Sawatzky, and J.W. Allen, Phys. Rev. Lett. **55**, 418 (1985).
  - [6] K. Knizek *et al.*, J. Phys.: Condens. Matter **18**, 3285 (2006); R. Radwanski and Z. Ropka, Sol. State Commun. **112**, 621 (1999); R. Radwanski and Z. Ropka, Physica B **281-282**, 507 (2000); Z. Ropka and R.J. Radwanski, Phys. Rev. B **67**, 172401 (2003).
  - [7] M. Medarde *et al.*, Phys. Rev. B **73**, 54424 (2006).
  - [8] L. Downward *et al.*, Phys. Rev. Lett. **95**, 106401 (2005).
  - [9] Y. Jiang *et al.*, Phys. Rev. B **76**, 224428 (2007).
  - [10] E.S. Bozin *et al.*, Phys. Rev. Lett. **98**, 137203 (2007).
  - [11] D. Louca and T. Egami, Phys. Rev. B **59**, 6193 (1999).
  - [12] N. Mannella *et al.*, Phys. Rev. Lett. **92**, 166401 (2004).
  - [13] V.G. Sathe *et al.*, J. Phys.: Condens. Matter **8**, 3889 (1996).
  - [14] D. Louca *et al.*, Phys. Rev. B **60**, 10378 (1999).
  - [15] D. Louca and J.L. Sarrao, Phys. Rev. Lett. **91**, 155501 (2003); D. Phelan *et al.*, Phys. Rev. Lett. **97**, 235501 (2006).
  - [16] V. Gnezdilov *et al.*, Low Temp. Phys. **32**, 162 (2006); G. Vanko *et al.*, Phys. Rev. B **73**, 24424 (2006); V.P. Plakhty *et al.*, J. Phys.: Condens. Matter **18** 3517 (2006);
  - [17] R.F. Klie *et al.*, Phys. Rev. Lett. **99**, 47203 (2007).
  - [18] A. Podlesnyak *et al.*, Phys. Rev. Lett. **97**, 247208 (2006); M.W. Haverkort *et al.*, Phys. Rev. Lett. **97**, 176405 (2006).
  - [19] S. Noguchi *et al.*, Phys. Rev. B **66**, 94404 (2002).
  - [20] V.V. Sikolenko *et al.*, J. Phys.: Condens. Matter **16**, 7313 (2004).
  - [21] C.H. Booth R-Space X-ray Absorption Package, <http://lise.lbl.gov/R SXAP>.
  - [22] A.L. Ankudinov *et al.*, Phys. Rev. B **58**, 7565 (1998).
  - [23] N.W. Ashcroft and N.D. Mermin, in Solid State Physics (Saunders College, Philadelphia, 1976).
  - [24] B.K. Teo, EXAFS: Basic Principles and Data analysis (Springer-Verlag, Ney York, 1986).
  - [25] P.A. Lee and G. Beni, Phys. Rev. B **15**, 2862 (1977); A. Bianconi, in *X-ray Absorption: principles, applications, techniques of EXAFS, SEXAFS and XANES*, edited by D. C. Koningsberger and R. Prins (John Wiley and Sons, New York, 1988), p. 594.
  - [26] V.V. Sikolenko *et al.*, Cryst. Rep. **51**, S67 (2006).
  - [27] O. Haas *et al.*, J. Solid State Chem. **177**, 1000 (2004); S.K. Pandey *et al.*, J. Phys.: Condens. Matter **18**, 10617 (2006).
  - [28] G. Maris *et al.*, Phys. Rev. B **67**, 224423 (2003).
  - [29] P.A. Lee, P.H. Citrin, P. Eisenberger and B.M. Kincaid, Rev. Mod. Phys. **53**, 769(1981).
  - [30] T. Egami and S.J.L. Billinge, *Underneath the Bragg Peaks: Structural Analysis of Complex Materials*, Pergamon Materials Series, Volume 7, (Pergamon, New York, 2003i).
  - [31] Th. Proffen *et al.*, Appl. Phys. **A74**, S163 (2002).
  - [32] P.F. Peterson *et al.*, J. Appl. Cryst. **33**, 1192 (2000).
  - [33] D. Phelan *et al.*, Phys. Rev. B **76**, 104111 (2007).
  - [34] D. Phelan *et al.*, Phys. Rev. Lett. **96**, 27201 (2006);

- [35] R. Caciuffo *et al.*, Phys. Rev. B **59**, 1068 (1999).
- [36] I.I. Mazin *et al.*, Phys. Rev. Lett. **98**, 176406 (2007).